

HADES and QCD phase diagram

Szymon Harabasz* for the HADES Collaboration

Technische Universität Darmstadt

E-mail: a.harabasz@gsi.de

We discuss new experimental results on the mechanisms of light nuclei production, fluctuations of conserved charges and the emissivity of matter, studied with HADES at SIS18. The multi-differential representations of hadron and dilepton spectra, collective effects and particle correlations are confronted with hitherto model calculations.

*CPOD2021 – International Conference on Critical Point and Onset of Deconfinement
15-19 March 2021
Online*

*Speaker.

1. Introduction

In heavy-ion collisions at center-of-mass energies per pair of colliding nucleons $\sqrt{s_{NN}} = 2 - 3$ GeV, transient states of QCD matter are produced, with the net-baryon density (equal in this case to the total baryon density) 2-3 times larger than the nuclear saturation density and temperatures between 50 and 70 MeV [1]. These conditions resemble the ones in neutron star mergers [2]. Their study will allow to constrain the nuclear equation of state (EoS) [3], after enough events are observed. In heavy-ion collisions, besides the opportunity to put additional constraints on the EoS, microscopic properties of the matter can be accessed.

Matter under such conditions is being studied with the High Acceptance Di-Electron Spectrometer (HADES) [4] at the heavy-ion synchrotron SIS18 in GSI, Germany. The physics program of the HADES experiment is focused on study of rare and penetrating probes in heavy-ion collisions, including electromagnetic probes and sub-threshold strangeness production. The experiment also studies collective effects and event-by-event fluctuations. Another pillar of the physics program are collisions of pion or nucleon beams with nucleon or nuclei targets. They provide not only reference measurements for heavy-ion collisions, but also allow to study properties of cold QCD matter and electromagnetic structure of baryons and hyperons.

This work will discuss mainly the results of the Au+Au run at $\sqrt{s_{NN}} = 2.42$ GeV in April 2012 and Ag+Ag run at $\sqrt{s_{NN}} = 2.55$ GeV (maximum allowed for Ag ions by SIS18 magnetic rigidity) and $\sqrt{s_{NN}} = 2.42$ GeV (identical to the previous Au run) in March 2019.

2. Experimental setup

The HADES setup (see the left panel of Fig. 1) has a six-fold rotational symmetry around the beam axis. It has nearly full acceptance in the azimuthal angle (except small gaps between the six sectors) and from 18 to 85 degree in the polar angle, which gives a good coverage of mid-rapidity for the incident beam energies available at SIS18, see the right panel of Fig. 1. Each sector is equipped with a lightweight tracking system consisting of four compact Multiwire Drift Chambers (MDCs): two in front and two behind the region of toroidal magnetic field generated by superconducting coils installed in the gaps between the sectors. Farther downstream with respect to the tracking system there are time-of-flight detectors: scintillator-based TOF at larger values of the polar angle and Resistive Plane Chambers (RPCs) closer to the beam axis, where their finer granularity allows to cope with higher particle density due to Lorentz boost in a fixed-target experiment. In the data taking campaigns before March 2019 the Pre-Shower detector was installed in the region behind RPC to support electron identification through a production of an electromagnetic cascade. After it has lost its performance due to aging, it has been replaced with a lead glass Electromagnetic Calorimeter (EMCal). It allows not only to directly detect photons, but also to identify electrons through a correlation of particle energy and momentum.

However, the main tool for lepton identification is the Ring Imaging Cherenkov (RICH) detector. It is filled with a radiator gas, in which, taking into account momenta of particles produced in the collisions at SIS18, practically only electrons can produce Cherenkov radiation. During the beam-times before March 2019, it was equipped with an MWPC-based photon detector, then

replaced with an array of photomultiplier tubes, which substantially improved its detection capabilities.

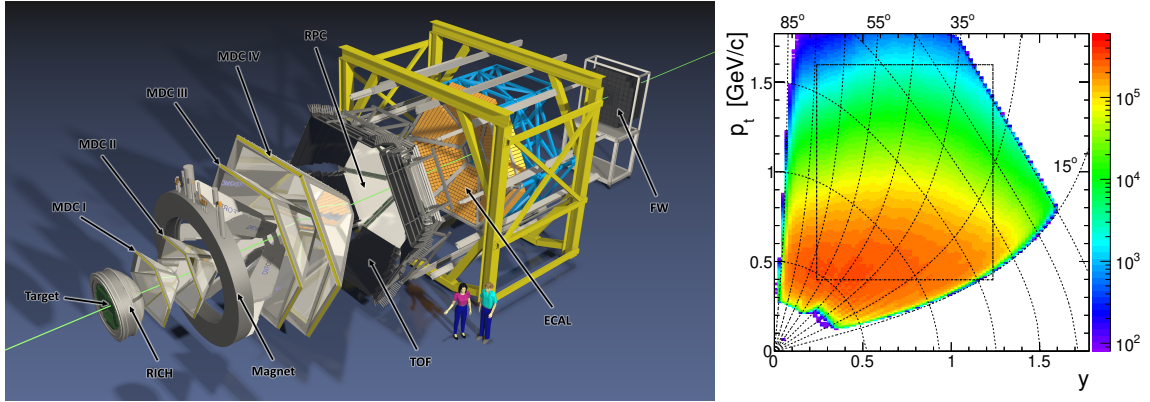


Figure 1: Left: 3D model of the HADES experimental setup, expanded along the beam axis for better visibility. Right: acceptance coverage for protons in Au+Au at $\sqrt{s_{NN}} = 2.42$ GeV (the dashed rectangle represents the phase space selection for the fluctuation analysis in [12], the thinner dashed curves correspond to constant momentum or θ angle of the values indicated at the end of selected curves).

Crucial are also a diamond counter START, which provides the reaction time T_0 with high precision, and Forward Wall – an array of plastic scintillator modules, used for the reconstruction of the reaction plane and for the determination of the event centrality.

3. Production of charged pions

At low-energy heavy-ion collisions charged pions play an important role, because these are the only newly produced particles, detected in the final state with relatively large abundance. This makes them a useful tool to constrain the properties of kinetic transport models and a relevant ingredient in determining the freeze-out properties of the system, either the chemical freeze-out via Statistical Hadronization Models or the kinetic one via Blast-Wave fits. Even the Coulomb potential and thus the size of the fireball can be deduced from the difference between momentum spectra of π^+ and π^- [5, 6].

Rapidity and transverse momentum distributions for π^- measured by HADES in Au+Au at $\sqrt{s_{NN}} = 2.42$ GeV are shown in Fig. 2, compared to state-of-the-art kinetic transport predictions, see [7] for more details and further references. One can observe that the rapidity spectra have different widths in different models, but experimental data are not sufficient to exclude any of them.

Light hadron spectra can also be compared to hydro-inspired models, where particles are generated according to the Cooper-Frye formula on an appropriately parametrized freeze-out hypersurface. In the most straightforward way, in the thermal distribution entering the Cooper-Frye formula, one can use thermodynamic parameters (temperature, chemical potentials, canonical suppression factors) obtained with Statistical Hadronization fits to ratios of particle yields. This amounts to assuming that the chemical freeze-out coincides with the kinetic one [8]. Example results for the source with spherical geometry and spherically-symmetric Hubble-like expansion are shown in Fig.

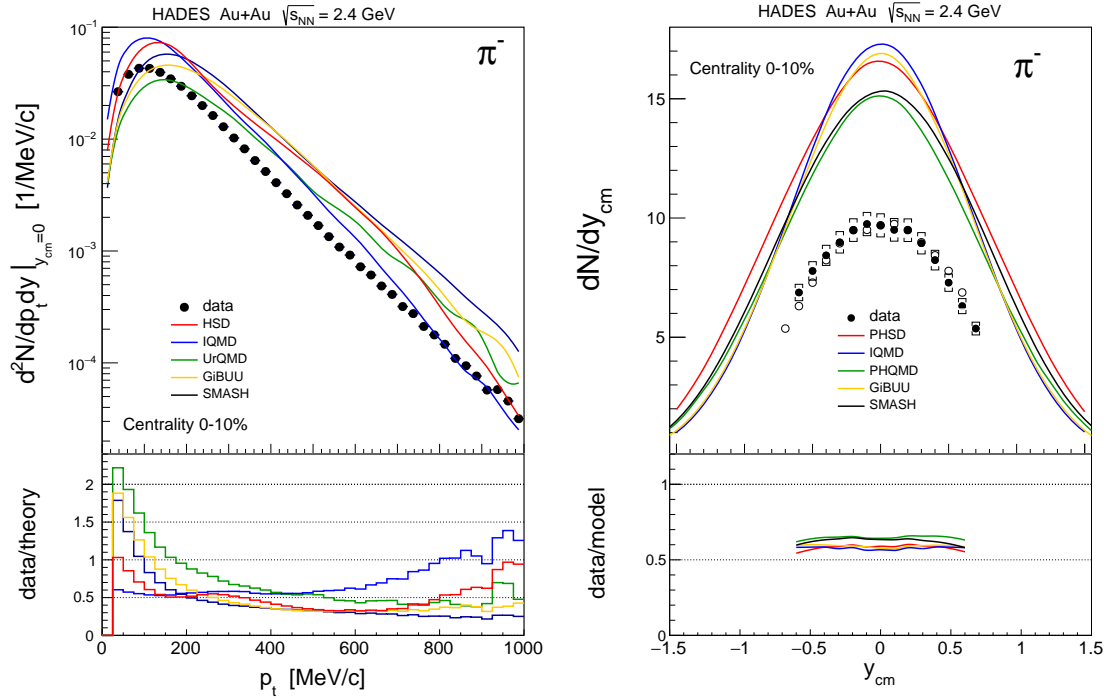


Figure 2: Transverse momentum (left) and rapidity (right) distributions of π^- measured in Au+Au collisions at $\sqrt{s_{NN}} = 2.42$ GeV, compared to different kinetic transport model calculations. Figures taken from [7], where references to the models can also be found.

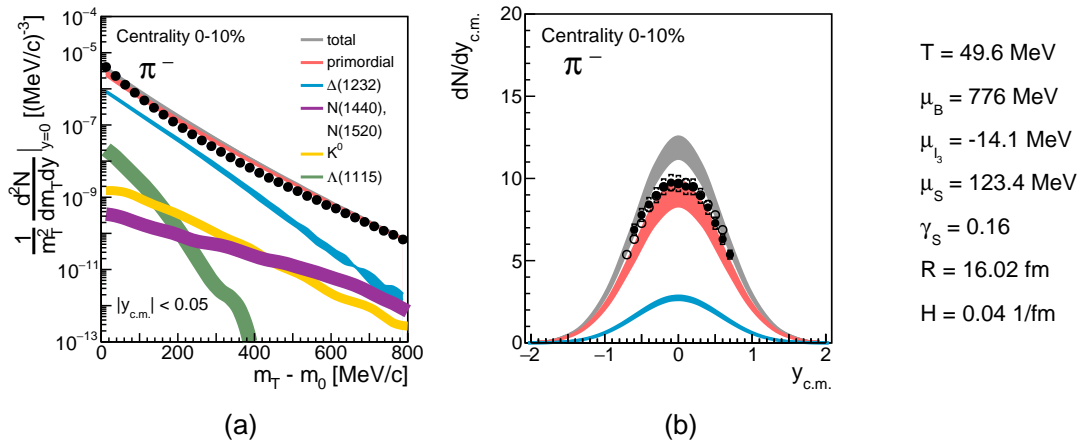


Figure 3: Transverse mass (a) and rapidity (b) distributions of π^- measured in 10% most central Au+Au collisions at $\sqrt{s_{NN}} = 2.42$ GeV, compared to a thermal model calculation from [9]. Bands represent systematic uncertainties of the model, thermodynamic parameters, total size of the fireball (R) and a constant H in the velocity parametrization of the Hubble-like expansion $\beta(r) = \tanh(Hr)$ are displayed on the right-hand side of the plots.

3. The model describes the data well taking into account its simplicity [9]. The fact that the rapidity distribution in the model is narrower in the data (their integrals are identical by construction) can be fixed by parametrizing fireball expansion profile to be spheroid instead of spherical.

4. Production and flow of light nuclei

HADES measures particles spectra and flow parameters in Au+Au collisions at $\sqrt{s_{NN}} = 2.42$ GeV [10]. The high precision of our measurements allows for a good sensitivity on the parameters of Skyrme potentials used in transport calculations and relate effectively to the equation of state.

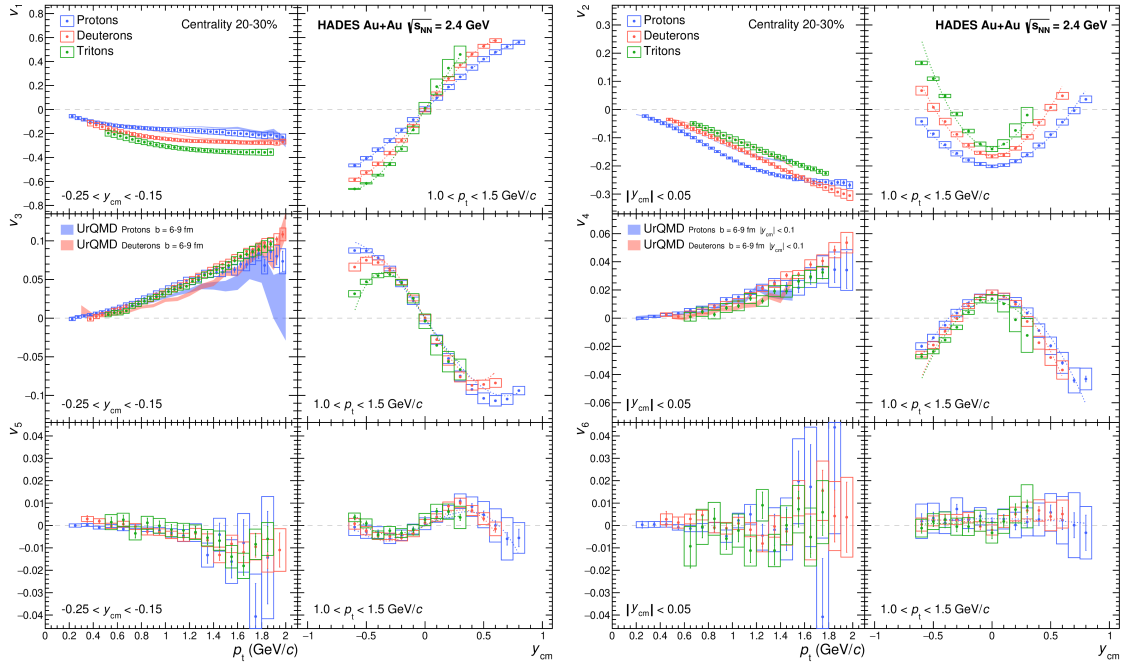


Figure 4: Azimuthal anisotropy $v_n, n = 1, \dots, 6$ of protons, deuterons and tritons measured in Au+Au collisions at $\sqrt{s_{NN}} = 2.42$ GeV [10], as a function of transverse momentum or rapidity, as indicated in the axis labels. Shaded areas for protons and deuterons are predictions from [11].

Especially sensitive to the equation of state are the Fourier harmonics of azimuthal distributions with respect to the reaction plane $v_n = \langle \cos(n(\phi - \Psi_{RP})) \rangle$, where ϕ is the azimuthal direction of particle momentum, Ψ_{RP} is the orientation of the reaction plane, and the average indicated by $\langle \cdot \rangle$ is over all particles (of a given specie) in all events. It is not trivial to describe with a given model Fourier coefficients of many orders, for several particle species and in various beam energies at the same time. To this end, strong constraints on the models, and equations of state used in them, can be put with the help of HADES data on v_n up to $n = 6$ for protons, deuterons and tritons, shown in Fig. 4.

5. Strangeness production

Both in Au+Au at $\sqrt{s_{NN}} = 2.42$ GeV and Ag+Ag at $\sqrt{s_{NN}} = 2.55$ GeV collisions various strange particles have been measured, including differential distributions and event centrality de-

pendence of the total yield. In the left and middle panels of Fig. 5 one can see examples of K_S^0 and Λ reconstructed via their weak decays in reactions of Ag+Ag at $\sqrt{s_{NN}} = 2.55$ GeV.

Center-of-mass energies per pair of colliding nuclei in heavy-ion collisions at SIS18 measured by HADES are below the threshold for production of any particles with strangeness. This so-called "sub-threshold strangeness production" occurs in part thanks to Fermi motion in colliding nuclei, in part by collecting in a series of particle-particle collisions the energy, which was initially brought to the system by more than one of the incident nucleons. In this context it is interesting to observe, that all the strange particles, despite having different production thresholds, follow nearly the same power-law dependence on the number of nucleons participating in the collision ($\langle A_{part} \rangle$, characterizing the event centrality), which only weakly depends on the collision system and energy, see the right panel of Fig. 5. This can be interpreted as the total number of produced strange quarks scale with the size of the fireball, but they can be freely redistributed between different hadron states. This could be understood if there are correlations in the system extending over many particles.

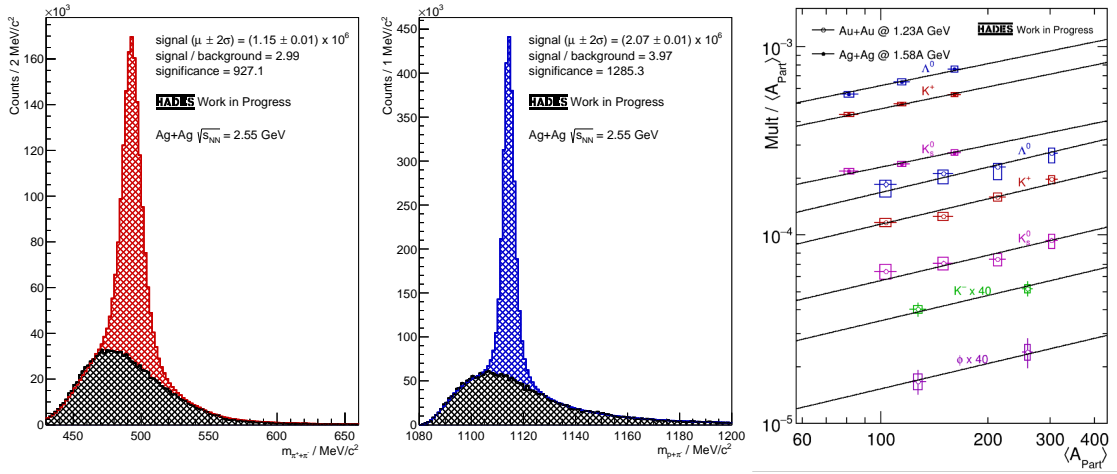


Figure 5: Left: invariant mass distribution of $\pi^+\pi^-$ pairs measured in Ag+Ag collisions at $\sqrt{s_{NN}} = 2.55$ GeV with cuts on a decay vertex optimized for the reconstruction of the K_S^0 meson. Middle: same for $p\pi^-$ pairs and the Λ baryon. The black areas in both plots represent combinatorial background obtained using the event mixing technique. Right: multiplicities of various strange particles, measured in Ag+Ag at $\sqrt{s_{NN}} = 2.55$ GeV (full symbols) and in Au+Au at $\sqrt{s_{NN}} = 2.42$ GeV (open symbols) as a function of mean number of nucleons participating in the collision $\langle A_{part} \rangle$; solid lines represent power-law fits, with exponent constrained to be the same for all particle species within one reaction.

6. Fluctuations of conserved charges

The behavior of QCD at high temperature and density can also be studied with the help of fluctuations of conserved charges within an appropriate region of the momentum space. In particular, the moments of multiplicity distributions should be sensitive to the non-monotonic behavior close to a first order phase transition and its critical end point. HADES measures momentum-integrated n -particle correlation functions [12]. They are shown in Fig. 6 as a function of mean proton number $\langle N_p \rangle$ for different event centrality classes. They scale as $|C_n| \propto \langle N_p \rangle^{\alpha_n}$ with $\alpha_2 = 1.86 \pm 0.04$, $\alpha_3 =$

2.84 ± 0.05 , $\alpha_4 = 3.89 \pm 0.14$ for 5% most central events. One possible interpretation of such an effect is the presence of long-range multi-particle momentum-space correlations.

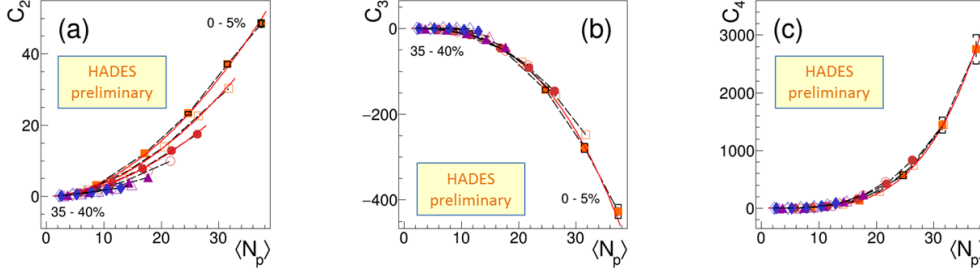


Figure 6: Multiparticle correlators as a function of mean proton number, plotted for eight 5%-wide event centrality classes (indicated by different markers). Error bars on the data points represent statistical uncertainty, cups – systematic ones (both shown only for 5% most central events).

This study will be further pursued with the new Ag+Ag data. Furthermore, an alternative approach to the data analysis, using the identity method of [13] will also be employed.

7. Dilepton production in Au+Au and Ag+Ag reactions

Another promising method to study strongly interacting matter is dilepton spectroscopy in heavy-ion collisions. Dileptons do not undergo strong interactions and the size as well as the life-time of the fireball are too small to make the effect of final-state electromagnetic interaction significant. Therefore, they probe whole evolution of the fireball, including its hot and dense stage. It can be accessed by subtracting contributions from first-chance NN collisions and hadrons decaying after the freeze-out. The former is represented by the properly normalized spectra from p+p and n+p collisions at the same energy, the latter by the simulated "cocktail", whose properties are fixed by the hadron measurements in the same Au+Au experiment. The resulting so-called excess yield is shown in Fig. 7, compared to two types of model calculations [15, 16, 17, 18, 19]. In the left panel these are vacuum ρ^0 distributions, which clearly fail to describe experimental data. Model curves shown in the right panel correspond to radiation of hot and dense medium and generally follow the trend visible in the experiment. Thus one can state that the ρ^0 meson gets "melted" in the medium.

In order to interpret the nature of radiation observed in Au+Au [20], reference measurements with proton and pion beams exploring electromagnetic structure of baryons are under way with HADES. In Ref. [22] the importance of the electromagnetic transition form factors of baryonic resonances in explaining the dilepton rates in pp collisions has been asserted.

The Vector Meson Dominance model is an essential ingredient of coarse-graining (CG in Fig. 7) calculations of thermal dilepton rates in Au+Au collisions. As discussed in [20], this approach better accounts for the observed melting of the ρ meson than the kinetic transport does.

High precision of the data will allow to devise a detailed interpretation of the comparison. To this end, HADES has collected dilepton data in Ag+Ag reactions at $\sqrt{s_{NN}} = 2.55$ GeV as well as $\sqrt{s_{NN}} = 2.42$ GeV. Invariant mass distribution in collisions at $\sqrt{s_{NN}} = 2.42$ GeV is shown in Fig. 8, compared to the simulated dilepton production channels emitting after the freeze-out, which

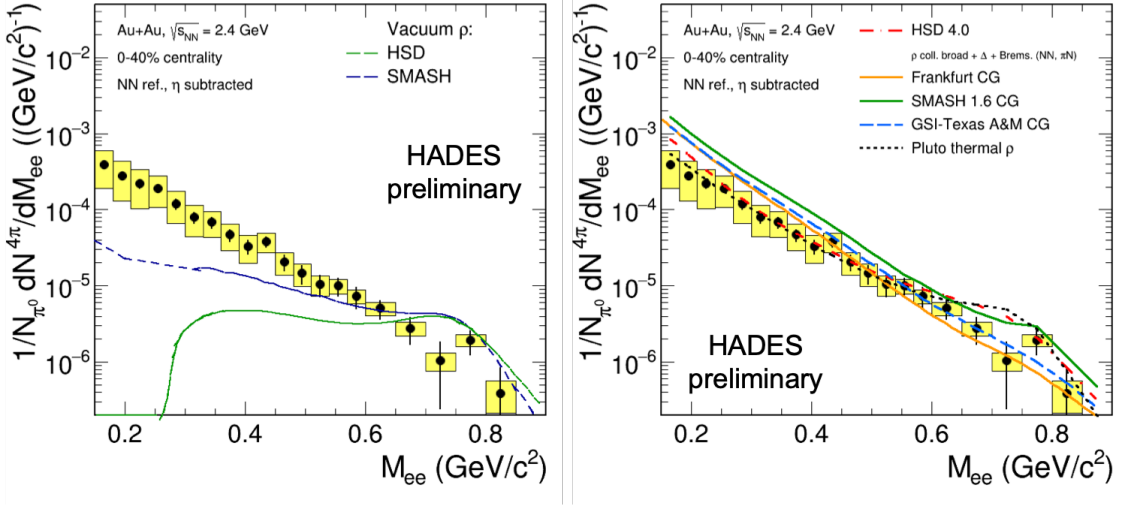


Figure 7: Invariant mass distribution of dileptons measured in Au+Au at $\sqrt{s_{NN}} = 2.42$ GeV after subtracting contributions from first-chance NN collisions, represented by p+p and n+p reactions measured at the same energy, and simulated η contribution from the freeze-out stage. Left: comparison to a simulated ρ^0 spectrum in the vacuum, right: contribution to various models of the hot and dense medium radiation.

by convention [21] are denoted "CocktailA". An excess radiation over the freeze-out sources is visible. As it can be concluded from the figure, at the lower collision energy, the statistics of signal pairs collected within just three days of data taking is comparable to the whole previous Au+Au run, thanks to the upgraded RICH detector. The statistics is about eight times larger at $\sqrt{s_{NN}} = 2.55$ GeV, where the data taking period was longer. In addition, improved efficiency of this detector allows for a detailed analysis of ring patterns and reject e^+e^- pairs with small opening angle, which correspond mainly to the external conversion of real photons, but contribute to the combinatorial background at all values of invariant mass. Thanks to this, the signal-to-background ratio can be reduced by a factor of at least 5, further increasing the statistical precision of the data.

With this data, systematic studies of energy, system-size and event centrality dependence of dilepton production in heavy-ion collisions at high μ_B will be performed. One can compare temperatures extracted from the slopes of the spectra of the in-medium contributions, like in [20] and total yields of these contributions, which can be related to the life-time of the system.

8. Summary

HADES provides a rich set of data from heavy-ion collisions in the few-GeV energy regime. Thanks to high interaction rate that can be handled by the detector, sufficient number of events have been collected in Au+Au and Ag+Ag to study statistics-hungry observables: dilepton spectra, azimuthal anisotropy coefficients v_n of protons, deuterons and tritons up to $n = 6$ or moments of event-by-event fluctuations. Also other quantities, like bulk properties extracted from hadron spectra, profit from large statistics and good acceptance coverage at mid-rapidity. With all this data, interesting observations were made. There is a tension between experimentally measured charged pion spectra and predictions from conventional kinetic transport model. Also the degree to which the cusp corresponding to the ρ^0 meson disappears in the dilepton data (resulting in the purely

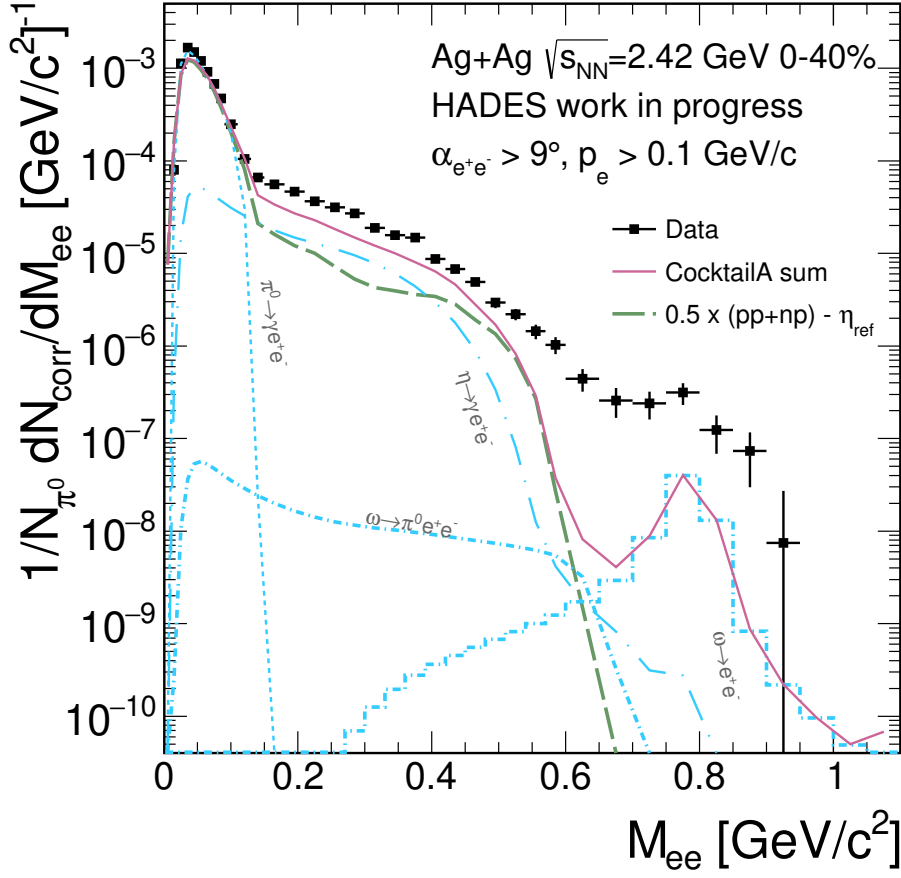


Figure 8: Invariant mass distribution of dileptons measured in Ag+Ag at $\sqrt{s_{NN}} = 2.42$ GeV, corrected for detection efficiency, but not extrapolated to the full phase space. Blue lines of different styles represent simulated "CocktailA" of dilepton production channels after the freeze-out, described by the labels in the figure. Their sum is plotted in addition with a pale violet red line. Properly normalized experimental spectrum measured in p+p and n+p collisions is plotted as long-dashed green curve.

thermal spectral shape) is not exactly reproduced by the kinetic transport and better results come from invoking the thermal rates for dilepton emission within a coarse-graining approach. The fact that centrality dependence of the yield is the same for all strange particle species is the same within a given collision system suggests, that strange quarks can be easily exchanged between hadrons and this points in the direction of long-range multi-particle correlations in the systems. In the same direction points also the approximate scaling $|C_n| \propto \langle N_p \rangle^n$ of n -particle correlation functions C_n .

New insights can be gained by comparing the same observables between Au+Au and Ag+Ag reactions, the latter measured at two slightly different collisions energies. In addition, one of HADES proposals for future beam-times, includes beam energy scan at SIS18, going below the maximum allowed by the magnetic rigidity of the synchrotron for Au ions. This may allow to observe the disappearance of hot and dense medium effects observed in the present data (by reducing the temperature and compression of the produced matter). It would be also possible to check how the fluctuation observables evolve when moving in the direction of the critical endpoint for the

nuclear liquid-gas phase transition.

Acknowledgements

This work has been supported by:
SIP JUC Cracow, Cracow (Poland), National Science Center, 2013/10/M/ST2/00042, 2016/23/P/ST2/04066 POLONEZ, 2017/25/N/ST2/00580, 2017/26/M/ST2/00600; TU Darmstadt, Darmstadt (Germany), VH-NG-823, DFG GRK 2128, DFG CRC-TR 211, BMBF:05P18RDFC1, HFHF; Goethe-University, Frankfurt (Germany), BMBF: 06FY9100I, BMBF:05P19RFFCA, GSI F&E, HIC for FAIR (LOEWE); Goethe-University, Frankfurt (Germany) and TU Darmstadt, Darmstadt (Germany), ExtreMe Matter Institute EMMI at GSI Darmstadt; TU München, Garching (Germany), MLL München, DFG EClust 153, GSI TMLRG1316F, BMBF 05P15WOFCA, SFB 1258, DFG FAB898/2-2; Russian Foundation for Basic Research (RFBR) funding within the research project no. 18-02-40086, National Research Nuclear University MEPhI in the framework of the Russian Academic Excellence Project (contract No. 02.a03.21.0005, 27.08.2013), Ministry of Science and Higher Education of the Russian Federation, Project "Fundamental properties of elementary particles and cosmology" No 0723-2020-0041; JLU Giessen, Giessen (Germany), BMBF:05P12RGGHM; IPN Orsay, Orsay Cedex (France), CNRS/IN2P3; NPI CAS, Rez, Rez (Czech Republic), MSMT LM2015049, OP VVV CZ.02.1.01/0.0/0.0/16 013/0001677, LTT17003.

References

- [1] T. Galatyuk *et al.*, Eur. Phys. J. A **52** (2016), 131
- [2] M. Hanauske *et al.*, Particles **2** (2019) no.1, 44-56
- [3] V. Dexheimer *et al.*, Universe **5** (2019), 129
- [4] G. Agakishiev *et al.* [HADES], Eur. Phys. J. A **41** (2009), 243-277
- [5] A. Wagner *et al.*, Phys. Lett. B **420** (1998) 20
- [6] D. Cebra *et al.*, arXiv:1408.1369
- [7] J. Adamczewski-Musch *et al.* [HADES], Eur. Phys. J. A **56** (2020) no.10, 259
- [8] W. Broniowski and W. Florkowski, Phys. Rev. Lett. **87** (2001), 272302
- [9] S. Harabasz *et al.*, Phys. Rev. C **102** (2020) no.5, 054903
- [10] J. Adamczewski-Musch *et al.* [HADES], Phys. Rev. Lett. **125** (2020), 262301
- [11] P. Hillmann *et al.*, J. Phys. G **47** (2020), 055101
- [12] J. Adamczewski-Musch *et al.* [HADES], Phys. Rev. C **102** (2020) no.2, 024914
- [13] A. Rustamov, M.I. Gorenstein, Phys. Rev. C **86** (2012) 044906
- [14] J. Adamczewski-Musch *et al.* [HADES], Eur. Phys. J. A **54** (2018) no.5, 85
- [15] S. Endres *et al.*, Phys. Rev. C **92** (2015) 014911
- [16] T. Galatyuk *et al.*, Eur. Phys. J. A, **52** (2016) no.5, 131
- [17] J. Staudenmaier *et al.*, Phys. Rev. C **98** (2018) 054908

- [18] E. Bratkovskaya *et al.*, Phys. Rev. C **87** (2013) 064907
- [19] I. Fröhlich *et al.*, J. Phys. Conf. Ser. **219** (2010) 032039
- [20] J. Adamczewski-Musch *et al.* [HADES], Nature Phys. **15** (2019) no.10, 1040-1045
- [21] G. Agakishiev *et al.* [HADES], Phys. Lett. B **663** (2008), 43-48
- [22] J. Adamczewski-Musch *et al.* [HADES], Phys. Rev. C **95** (2017) no.6, 065205